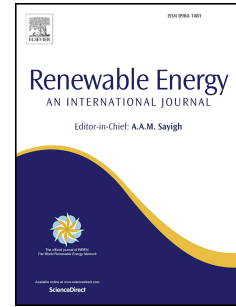


Accepted Manuscript

The T-I-G^{ER} method: A graphical alternative to support the design and management of shallow geothermal energy exploitations at the metropolitan scale

Mar Alcaraz, Luis Vives, Enric Vázquez-Suñé



PII: S0960-1481(17)30203-3

DOI: [10.1016/j.renene.2017.03.022](https://doi.org/10.1016/j.renene.2017.03.022)

Reference: RENE 8615

To appear in: *Renewable Energy*

Received Date: 22 August 2016

Revised Date: 6 March 2017

Accepted Date: 8 March 2017

Please cite this article as: Alcaraz M, Vives L, Vázquez-Suñé E, The T-I-G^{ER} method: A graphical alternative to support the design and management of shallow geothermal energy exploitations at the metropolitan scale, *Renewable Energy* (2017), doi: 10.1016/j.renene.2017.03.022.

This is a PDF file of an unedited manuscript that has been accepted for publication. As a service to our customers we are providing this early version of the manuscript. The manuscript will undergo copyediting, typesetting, and review of the resulting proof before it is published in its final form. Please note that during the production process errors may be discovered which could affect the content, and all legal disclaimers that apply to the journal pertain.

1 **THE T-I-G^{ER} METHOD: A GRAPHICAL ALTERNATIVE TO SUPPORT THE**
 2 **DESIGN AND MANAGEMENT OF SHALLOW GEOTHERMAL ENERGY**
 3 **EXPLOITATIONS AT THE METROPOLITAN SCALE¹**

4 **Mar Alcaraz^{a,b*}, Luis Vives^{a,c}, Enric Vázquez-Suñé^{d,e}**

5 ^a Instituto de Hidrología de Llanuras “Dr. Eduardo Usunoff”.

6 República de Italia, 78. B7300 Azul, Provincia de Buenos Aires, Argentina.

7 ^b Consejo Nacional de Investigaciones Científicas (CONICET).

8 Av. Rivadavia, 1917. C1066AAJ Ciudad Autónoma de Buenos Aires, Argentina.

9 ^c Universidad Nacional del Centro de la Provincia de Buenos Aires (UNICEN).

10 Av. Gral. Pinto, 399. B7000GHG Tandil, Argentina, Provincia de Buenos Aires.

11 ^d Institute of Environmental Assessment and Water Research (IDÆA-CSIC).

12 Jordi Girona 18, 08034 Barcelona, Spain

13 ^e Associated Unit: Hydrogeology Group (UPC-CSIC)

14
 15 * Corresponding author. Tel./Fax: +54 2281 432666.

16 E-mail address: malcaraz@faa.unicen.edu.ar (Mar Alcaraz).

17 Postal address: Av. República de Italia, 780. B7300 Azul, Provincia de Buenos Aires

18 **Abstract:**

19 The number of shallow geothermal exploitations is growing without a
 20 widespread technical framework for this energy resource to be sustainably allocated
 21 between users. The thermal impacts that are produced by neighboring exploitations can
 22 deplete the resource if they are not properly distributed.

23 Therefore, we present an accessible and simple methodology to define the
 24 maximum potential that can be extracted and the position of the exploitations with the
 25 objective of limiting the thermal impacts to the available space.

26 The proposed method, named T-I-G^{ER}, takes into account the hydraulic and
 27 thermal properties of the subsurface as well as the size and orientation of the owner’s
 28 plot. All this information is integrated in two different graphs: the thermal characteristic
 29 curve and the thermal plume graph. Therefore, the installer is able to graphically define
 30 the maximum potential and to check that thermal influences are restricted to the plot
 31 area.

32 We show with a hypothetical application in Azul city, Argentina, that the
 33 maximum extraction potential from similar plots can vary depending on the orientation
 34 of the plots with respect to groundwater flow. In the plots where the major dimension is
 35 parallel to groundwater flow, the maximum potential can be approximately twice the
 36 potential of the perpendicular plots.

37 **Keywords:** low-enthalpy geothermal energy, borehole heat exchanger, thermal
 38 characteristic curve, thermal contamination.

39
 1 **Acronyms:**

SGE: Shallow Geothermal Energy

TCC: Thermal Characteristic Curve

SGP: Shallow Geothermal Potential

TPG: Thermal Plume Graph

BHE: Borehole Heat Exchanger

40 1 INTRODUCTION

41 As a consequence of the world-wide concern on climate change, national
42 legislations have been modified to implement measures to sustainably meet energy
43 needs [1], [2]. This results in an increase in private initiatives and investments on
44 renewable energies, which are exponentially growing in an effort to reduce greenhouse
45 gas emissions. Consequently, renewable energies have been experiencing a boom in
46 recent years.

47 The advantages of shallow geothermal energy (SGE), such as its ubiquity and
48 independence of weather conditions [3], compared to other renewable energies make
49 SGE a feasible option to certain stakeholders. Despite its advantages, the success and
50 spreading of this technology [4] are highly dependent on sociological and cultural
51 aspects, as suggested by [5], partly due to economic factors. To promote the
52 exploitation of SGE, the authorities in charge should ensure the long-term efficiency of
53 these installations through sustainable resource management.

54 SGE is stored in the ground up to 400 m in depth. It is usually exploited with
55 borehole heat exchangers (BHE) coupled with heat pumps, among other configurations
56 [6]. A liquid, which can have enhanced thermal properties or simply be water, is
57 recirculated inside the BHE where the energy is extracted from or dissipated in the
58 ground and transferred to the heat pump.

59 Although SGE is a renewable energy, it is a limited energy resource that can be
60 overexploited [7]. The efficiency and sustainability of BHEs rely on both the BHE
61 being produced and any neighboring BHE [8].

62 On the one hand, sizing of the BHEs based on the geological, hydrogeological
63 and geothermal properties of the subsurface is required to produce the suitable potential,
64 according to the thermal restoration capacity of the subsurface. This would ensure
65 efficiency during the producible life of the proposed BHE [9].

66 On the other hand, nearby exploitations can affect the optimal performance of
67 the BHE through their thermal plumes [10]. A thermal plume is the thermal
68 contamination that occurs in the subsurface due to the extraction or dissipation of heat
69 with the BHEs. The size and intensity of thermal plumes depend on different variables,
70 such as the extracted shallow geothermal potential (SGP), the groundwater velocity and

71 other thermal parameters (i.e., thermal conductivity, heat capacity and thermal
72 dispersion). These thermal plumes are ultimately responsible for depleting SGE
73 resources and should be controlled.

74 Moreover, the subsurface exploitation of SGE conflicts with other subsurface
75 resources. Currently, the first steps towards the holistic management of the urban
76 subsurface are beginning to be defined [11]–[13]. Nevertheless, the instruments to
77 implement these steps, especially those related to SGE management, are not sufficiently
78 developed nor applied.

79 The lack of applied management methodologies that consider the above-
80 mentioned aspects is leading to thermal interferences between exploitations [14] and,
81 consequently, to efficiency losses. The administration responsible for SGE management
82 only defines maximum distance thresholds between SGE exploitations [15]. At most,
83 more advanced geological and hydrogeological studies are required by administrators
84 when the potential production exceeds a limit. However, this is not the case for
85 individual BHEs [16]. The BHE installer is responsible for ensuring the long-term
86 efficiency of the exploitations, which implies that BHE sizing for the exploitation
87 should take into account its relationship with neighboring exploitations. One of the
88 advantages of SGE production, its null visual impact, becomes a disadvantage if no
89 records for current SGE exploitations are available. Therefore, a level of uncertainty
90 must be assumed when sizing new BHEs due to the uncertainty of the thermal
91 environment in the subsurface.

92 Existing SGE management methodologies are based on numerical modeling.
93 They require a comprehensive understanding of the thermal system over the entire city.
94 These models must represent the complex thermal relationships between all of the
95 subsurface entities, which represent heat sources or sinks, such as existing BHEs or
96 wastewater network pipes [17]. These tools cannot be extensively used due to two main
97 problems: the complexity during definition of conceptual geothermal models and the
98 scarcity of highly qualified staff to construct, maintain and operate such numerical
99 models. These disadvantages make it difficult to widely implement numerical models,
100 so they are relegated to mature SGE markets where adequate information for the
101 thermal state of the subsurface and exploitation data are available [18]–[20]. In contrast,
102 for young SGE markets with incipient exploitation development, more accessible and
103 simple methodologies are required to manage SGE production.

104 Among these alternative methodologies, those based on the quantification of
105 SGP are highly developed. Usually, geographical information systems (GIS) technology
106 is typically applied to create maps with SGP distribution [21]–[25] and an initial
107 estimate of thermal influence [26]. Progressively, GIS methodologies have started to
108 reduce the scale of work and take into account additional variables such as urban
109 planning and population density [27], [28].

110 However, there is still a need to provide more accessible tools and
111 methodologies to installers who are in charge of designing SGE exploitations. Their
112 responsibility to guarantee a long efficiency life should be supported by reliable and
113 accessible tools that account for the geological, hydrogeological and geothermal
114 subsurface properties and include the uncertainties of the thermal behavior of
115 groundwater. Existing commercial and non-commercial tools support the definition of
116 BHEs' properties (such as its length) based on the subsurface thermal properties [29]
117 and the BHE performance [30], without considering the thermal impacts on the aquifer.
118 To overcome this gap, this study presents a methodology based on a graphical solution
119 named the T-I-G^{ER} (Thermal Impacts Graph^{ER}) method. It is based on two different
120 graphs that represent the thermal contamination in the subsurface: the thermal
121 characteristic curve (TCC) and the thermal plume graph (TPG). These graphs can be
122 easily created and applied by the BHE installers.

123 The structure of the paper is as follows. In Section 2 the T-I-G^{ER} method is
124 introduced, describing the main concepts and inputs required. In Section 3, a
125 hypothetical example of the proposed methodology is presented for the city of Azul,
126 Argentina, whose climate, subsurface and urban characteristics could make it a case
127 study in Argentina for SGE production. Finally, conclusions are included in Section 4.

128 **2 T-I-G^{ER} METHOD**

129 In this section, the mathematical basis of the T-I-G^{ER} is method is presented,
130 along with the definition of its two innovative graphs and a description of the
131 information required for implementing this method.

132 **2.1 Underlying theory**

133 The thermal behavior can be simulated with the heat transport equation in
134 porous media [31]:

$$135 \quad \rho c \frac{\partial T}{\partial t} + q \rho_w c_w \frac{\partial T}{\partial x} - \lambda_x \frac{\partial^2 T}{\partial x^2} - \lambda_y \frac{\partial^2 T}{\partial y^2} - S = 0 \quad (1)$$

136 where T is the temperature as the state variable (K), q is the groundwater
 137 velocity, also known as Darcy velocity (m/s), ρc and $\rho_w c_w$ are the volumetric heat
 138 capacity of the subsurface and water ($J/m^3/K$), respectively, $\lambda_{x/y}$ is the effective thermal
 139 conductivity in the longitudinal and transverse directions ($W/m/K$), x/y are the Cartesian
 140 coordinates, t is the time (s) and S is the heat source/sink term (W/m^3).

141 Eq. (1) has been solved under different boundary conditions [32]. [33] proposed
 142 the following analytical solution for this differential equation in the transient state:

$$143 \quad \Delta T(x, y, t) = \frac{q_L}{4 \pi \sqrt{\lambda_x \lambda_y}} \exp\left[\frac{\rho_w c_w q}{2 \lambda_x} x\right] \int_0^{\frac{(\rho_w c_w)^2 t}{4 \rho c \lambda_x}} \exp\left[-\phi - \left(\frac{x^2}{\lambda_x} + \frac{y^2}{\lambda_y}\right) \frac{(\rho_w c_w q)^2}{16 \lambda_x \phi}\right] \frac{d\phi}{\phi} \quad (2)$$

144 where ϕ is the integration variable, ΔT is the temperature change produced in the
 145 ground (K) and q_L is the heating rate or SGP (W/m). This last variable is the gross SGP
 146 extracted from the subsurface, without considering the loss of energy during SGE
 147 production.

148 Eq. (2) is based on the moving infinite line source model (MILS) and takes into
 149 account the thermal dispersion heat transport mechanism. It includes the presence of
 150 groundwater flow through the advection and dispersion heat transport mechanisms. This
 151 solution applies for an infinite, homogeneous and isotropic domain in a uniform
 152 groundwater velocity field where a heat source/sink is conceptualized as an infinite line.

153 The MILS has been previously applied by [26], [34]–[36] to represent the
 154 thermal behaviour of groundwater under the influence of the BHE. Moreover, it has
 155 been validated for the standard variable range of geological properties in [26].

156 **2.2 T-I-G^{ER} graphs**

157 The following two graphs represent the characteristics of the thermal plumes
 158 produced by the BHE. They both support the decision making process when defining
 159 and managing SGE exploitations; the optimal SGP and the position of the BHE can be
 160 established based on the thermal impacts on the subsurface. Additional information
 161 must be considered based on the specific characteristics of the site when exploiting

162 SGE, to avoid undesirable consequences [37], [38]. Such specifications are not
163 considered by the T-I-G^{ER} method.

164 2.2.1 The Thermal Characteristic Curve (TCC)

165 The T-I-G^{ER} method is based on the thermal characteristic curve (TCC), which
166 was previously introduced in [28]. The TCC graphically represents the thermal behavior
167 of the subsurface media when SGE is being exploited by a BHE. It is an SGP vs.
168 thermal plume size (length x and width y) graph, i.e., the TCC represents q_L vs x, y . A
169 synthetic TCC is shown in **Figure 1**.

170 Eq. (2) can be reformulated to obtain an expression in the form of $q_L = f(x)$,
171 Eq. (3), to represent the thermal plume length. The thermal plume width is represented
172 with an expression in the form of $q_L = f(y)$, Eq. (4). Both expressions are implemented
173 to create the TCC. These expressions are formed by setting the opposite coordinate to
174 zero:

$$175 \quad q_L = f(x, y = 0) = \frac{\Delta T 4\pi \sqrt{\lambda_x \lambda_y}}{\exp\left(\frac{q \rho_w c_w x}{2\lambda_x}\right) \int_0^{\frac{(\rho_w c_w)^2 t}{4 \rho c \lambda_x}} \frac{1}{\varphi} \exp\left(-\varphi - \left(\frac{x^2}{\lambda_x}\right) \frac{(q \rho_w c_w)^2}{16 \lambda_x \varphi}\right) d\varphi} \quad (3)$$

$$176 \quad q_L = f(x = 0, y) = \frac{\Delta T 4\pi \sqrt{\lambda_x \lambda_y}}{\int_0^{\frac{(\rho_w c_w)^2 t}{4 \rho c \lambda_x}} \frac{1}{\varphi} \exp\left(-\varphi - \left(\frac{y^2}{\lambda_y}\right) \frac{(q \rho_w c_w)^2}{16 \lambda_x \varphi}\right) d\varphi} \quad (4)$$

178 The TCC can be used for two different approaches. First, if the available area
179 inside the plot is known, the optimal SGP can be determined by the TCC. Conversely,
180 assuming that the SGE production is known, the TCC determines the size of the thermal
181 plume produced by the BHE.

182 Additionally, the TCC offers information related to the maximum SGP that can
183 be extracted without increasing the temperature more than 10 K at the BHE wall
184 (**Figure 1**).

185 **2.2.2 The Thermal Plume Graph (TPG)**

186 To determine the shape of thermal plumes when defining the BHE position, a
187 second graph is presented to complement the TCC. It contains the length and width of
188 the thermal plume, the position of the maximum width and the upstream and
189 downstream distance from the BHE (**Figure 2**).

190 The TPG is drawn from Eq. (2). The isothermal line can be determined by the
191 inversion of $\Delta T = f(x, y)$. This expression represents the set of points (x, y) that defines
192 the thermal plume. The inversion is performed numerically to state y as a function of x .

193 With the TPG, the installer is able to locate the BHE inside the cadastral plot to
194 maintain the thermal contamination inside the plot. This graph depends on the hydraulic
195 and thermal properties of the cadastral plot (like the TCC) but also depends on the SGP
196 that would be produced with the BHE. Therefore, each BHE inside a cadastral plot will
197 need a different TPG.

198 **2.3 Required information**

199 The T-I-G^{ER} method includes two different working scales: on the larger
200 metropolitan scale, the local authorities should define regulation parameters to restrict
201 the SGE exploitation (named constraining variables) and should accomplish the
202 elementary studies for the geological and hydrogeological properties of the city to
203 provide the initial data; on the smaller plot scale, the installer is responsible for sizing
204 the SGE exploitation. For each scale, the responsible agents and the temporal scales are
205 different, i.e., they have different participation frequencies. While the local
206 administration only has to participate, e.g., once every five years to generate and update
207 the regional information, the installers participate at every SGE site.

208 The first step in the proposed methodology is performed by the local
209 administration, which must provide the required data at the metropolitan scale. These
210 data are predominantly standard and are typically available due to previous studies
211 related to groundwater management, so it is not necessary to generate new data
212 specifically for SGE management.

213 Once the regional data has been provided by the local administration, the
214 installer has to consider the specific characteristics of the cadastral plot to ensure the
215 efficiency and high performance of the SGE exploitation. The working scale in this step
216 is reduced. The installer must focus on the site-specific cadastral plot.

217 **2.3.1 Hydraulic and geothermal characterization of the subsurface**

218 Groundwater presence is a determinant factor in the efficiency and the recovery
219 of SGE exploitations [36], [39]; therefore, a hydrogeological study must be performed.
220 Moreover, the piezometric surface and the hydraulic conductivity are common outputs
221 from a general hydrogeological study. This information can be used to generate the
222 groundwater velocity field of the exploited aquifer by applying Darcy's Law:

$$223 \quad q = K \cdot i \quad (5)$$

224 where q is the Darcy velocity or groundwater velocity (m/s), K is the hydraulic
225 conductivity (m/s) and i is the hydraulic gradient. The slope of the piezometric surface
226 can be calculated using inherent GIS tools to determine the hydraulic gradient field.

227 The direction of groundwater velocity will also be of interest to constrain the
228 thermal contamination to the available space. The groundwater flow net indicates this
229 aspect and can also be defined from the piezometric surface. The equipotential (i.e.,
230 piezometric lines) and flow lines describing the groundwater flow net can be created
231 using standard GIS tools.

232 Ideally, geothermal variables (i.e., thermal conductivity, volumetric heat
233 capacity and thermal dispersion) should be obtained from field studies. However, they
234 can be obtained from the literature without introducing too much error on the estimation
235 if groundwater is present due to the small range of variation of geothermal variables
236 compared with the variable range of groundwater velocity [40]. Groundwater velocity
237 varies by several orders of magnitude (e.g., from 10^{-5} m/s to 10^{-8} m/s for sedimentary
238 aquifers), so it has much more relevance than geothermal parameters on the final
239 estimation of SGP and thermal impacts.

240 **2.3.2 Constraining variables**

241 To create the TCC, additional information must be defined by the administrator:
242 the constraining variables ΔT and t . The uncertainties about the geological,
243 hydrogeological and geothermal models can be considered by adjusting the values of
244 both constraining variables. More conservative values of these variables should be
245 assumed if no reliable studies are available.

246 The temperature change, ΔT , represents the threshold upon which local
247 administration will consider that thermal contamination is produced. The more reliable
248 the conceptual model describing the thermal behavior of the subsurface is, the higher is

249 the ΔT value. The thermal plume encloses an area where the BHE produces a
250 temperature change greater than ΔT .

251 The constraining variable t represents the elapsed time since the start of the BHE
252 operation. It depends on how long the BHE is working in the cooling or heating mode.
253 The longer period should be selected.

254 When creating the TCC, it is required that both constraining variables, ΔT and t ,
255 are established by the local administration. Thus, the administration can regulate the
256 density of SGE exploitations according to the existing geological and hydrogeological
257 knowledge of the area.

258 **2.3.3 Urban planning and limiting plot dimensions**

259 To avoid thermal interferences between exploitations, the thermal plume must be
260 contained inside the available surface, i.e., the owner's cadastral plot. The cadastral plot
261 distribution is usually provided by local authorities, and it is usually available online
262 through web map services.

263 Next, the installer must first determine the feasible areas inside the cadastral plot
264 to drill the BHE. The installer must consider the existence of underground
265 infrastructures and facilities, such as electricity or water supply network pipes, and the
266 accessibility of the borehole drilling rig.

267 When the feasible areas for drilling have been demarcated, the installer has to
268 overlap these areas with the groundwater flow nets. The installer defines the maximum
269 dimensions (length and width) available inside the cadastral plot according to the
270 groundwater flow net. The maximum length and width should be parallel and
271 perpendicular to groundwater flow lines, respectively, to obtain higher SGP values. The
272 orientation of the cadastral plot dimensions must concur with the groundwater flow
273 lines to optimize the SGE exploitation (**Figure 3**). These dimensions limit the size of
274 the thermal plume and, hence, the SGP that can be exploited.

275 The maximum length, denoted as L , defines the maximum extent of the thermal
276 plume produced by a BHE. It includes both the distances downstream and upstream of
277 the BHE. The maximum width, denoted as W , establishes the maximum breadth of the
278 thermal plume at both sides of the longitudinal thermal plume axis. These dimensions, L
279 and W , will characterize the cadastral plot and can be obtained with standard GIS tools.
280 They support the definition of the maximum SGP that can be extracted in a sustainable

281 manner based on the thermal characteristic curve (TCC). In a cadastral plot whose
282 larger dimension is parallel to groundwater flow, such as Plot A shown in **Figure 3**, the
283 SGP would be greater than in a cadastral plot perpendicular to groundwater flow (Plot B
284 in **Figure 3**).

285 **3 APPLICATION**

286 **3.1 General settings**

287 The city of Azul is located in the middle of the Buenos Aires province, in the La
288 Pampa region (**Figure 4**). It is characterized by a humid subtropical climate, with an
289 average precipitation of 960 mm/y and an annual average temperature of 14°C. Azul
290 city is located in the Del Azul Creek basin, from which it is named. The regional
291 geological and hydrogeological properties are described in [41].

292 Drinking water is produced in the town from groundwater resources, so the
293 subsurface system is well studied and controlled in this area. Several geological and
294 hydrogeological analyses had been conducted for the study area at a local scale [42],
295 [43]. However, they are mostly related to the hydraulic behavior, while the thermal
296 properties have not been studied.

297 The main hydrogeological unit is the Pampeano aquifer, which encompasses
298 both Postpampeano and Pampeano sediments (Pleistocene-Holocene age). They are
299 composed of silts, sandy silts and clayey silts. Underlying these sediments is the
300 Precambrian basement, between 111 and 143 m depth.

301 Especially relevant in this area is the generalized problem of high levels of
302 arsenic in the groundwater [44], [45]. As suggested by [46], the SGE exploitation could
303 induce arsenic mobility. As a result, public administration should control the chemical
304 and physical properties of groundwater during exploitation of SGE to ensure safety,
305 especially if the exploited aquifer is used for the production of drinking water, as is the
306 case for Azul city.

307 **3.2 Input data**

308 **3.2.1 Geothermal parameters**

309 The thermal properties obtained from existing studies and literature [40] are
310 shown in **Table 1**.

311 **Table 1.** Hydraulic and thermal properties considered for the underground media in Azul city.

Parameter	Value	Unit
Thermal conductivity	2.7	W/m/K
Volumetric Heat Capacity	$2.8 \cdot 10^6$	J/m³/K
Thermal dispersion	10/1	m

312 **3.2.2 Groundwater velocity and flowlines**

313 The hydraulic conductivity of the main aquifer in Azul city is $5.8 \cdot 10^{-5}$ m/s.
 314 **Figure 5** shows the piezometric surface in the area and the groundwater velocity field
 315 derived from it according to Eq. (5). These hydraulic properties were obtained from
 316 [43].

317 **3.2.3 Constraining variables**

318 In the case of Azul city, intermediate conservative values of ΔT and t can be
 319 assumed due to the reliable knowledge of the geology and hydrogeology. The
 320 performance of the in situ thermal tests to estimate thermal dispersion would lead to
 321 more flexible values of both constraining variables. Their values are shown in **Table 2**.
 322 The lower the ΔT value, the bigger the thermal plumes, so the number of BHEs allowed
 323 would be reduced. The influence of the elapsed time depends on the temporal evolution
 324 of the system: the longer the t value, the bigger the thermal plumes, until the steady
 325 state is reached, when the thermal plume would not grow larger.

326 **Table 2.** Constraining variables values that are required to construct the TCC.

Constraining Variable	Value	Unit
Temperature increment, ΔT	0.5	K
Elapsed time, t (6 months)	15552000	s

327 **3.2.4 Urban planning and limiting plot dimensions**

328 The Azulean population is over 60.000 inhabitants, and its urbanization is
 329 primarily horizontal, with single-family attached homes. The blocks of Azul city are
 330 shown in **Figure 5**. The blocks are usually square, with sides of 100 m long, and
 331 divided into 20 cadastral plots on average with irregular distributions [47].

332 In this work, the possibilities of SGE exploitation were analyzed for urban block
 333 186 shown in **Figure 6**. The proposed block is divided into 22 cadastral plots. The
 334 optimal plots for SGE exploitations are those oriented in the direction of groundwater
 335 flow. In this work, two plots with similar areas and different orientations will be
 336 analyzed in order to evaluate the consequences of the groundwater flow direction. The
 337 limiting dimensions for each cadastral plot are shown in **Figure 6**.

338 3.3 RESULTS

339 At this stage, the TCC must be available with the objective to define the SGP
340 and the position of each BHE. Ideally, the public administration should provide the
341 TCC and the shape of the thermal plume through an online web map application. If this
342 is not the case, the installer could create them with the Python scripts available as
343 supplementary material.

344 3.3.1 Shallow geothermal potential (SGP)

345 At this point, the TCC can answer two questions: if the energy demand that must
346 be satisfied with SGE is known, the suitability of SGE exploitation can be defined. The
347 TCC indicates the length and width of the thermal plume; if these dimensions can be
348 accommodated inside the cadastral plot, then the SGE exploitation would be feasible.
349 The maximum SGP that can be exploited can also be obtained from the TCC. The TCC
350 returns a value of SGP for dimension L and a different value for dimension W . The
351 smaller of the two values indicates the potential that can be exploited.

352 Cadastral plots 15 and 5 share the hydraulic and thermal properties that define
353 the TCC. In this situation, the same TCC can be used for both plots which is shown in
354 **Figure 7**. The TCC indicates that the maximum SGE potential for one BHE is 89 W/m.
355 However, the thermal plume size produced by this maximum SGP ($L = 23$ m and $W =$
356 14 m) is greater than the available space in both cadastral plots; therefore, it is necessary
357 to define smaller SGP values for both plots.

358 The limiting dimension of cadastral plot 15 is $W = 10$ m. According to the TCC,
359 the SGP that can be extracted from one BHE in this plot is 40 W/m. For cadastral plot 5,
360 the SGE potential that can be extracted is 21 W/m, corresponding to $L = 10$ m, which is
361 the limiting dimension of this plot (**Figure 7**).

362 3.3.2 Allocation of BHEs according to thermal contamination

363 Each BHE defined previously with different SGPs has its own TPG. Therefore,
364 two TPGs are created to support the allocation of the BHEs. They are shown in **Figure**
365 **8**.

366 The thermal contamination can be manually drawn from the TPG as shown in
367 **Figure 9**. The characteristics of cadastral plot 15 would allow two BHEs inside the
368 available space. For standard BHEs of 115 m depth, the total SGP that could be
369 extracted from cadastral plot 15 would be 2×115 (m) \times 40 (W/m) = 9.2 kW.

370 The orientation of cadastral plot 5 with respect to groundwater flow direction is
371 not efficient to extract SGE. This implies that a very low SGP could be extracted
372 without thermally affecting the neighboring plot (21 W/m). To obtain approximately the
373 same SGP from this plot, four BHEs would be required: $4 \times 115 \text{ (m)} \times 21 \text{ (W/m)} = 9.6$
374 kW.

375 Other configurations are possible by varying the number of boreholes and the
376 limiting dimensions, but in this work, the standard criterion is to adjust the number of
377 BHEs. The installer could try different configurations of the BHE length and number to
378 obtain the required SGP.

379 3.3.3 Comparison with a reference scenario

380 To compare the determined results, an alternative scenario is proposed to use as
381 a reference. Recommendations of existing Spanish regulations are considered, as there
382 are no applicable regulations related to SGE in Argentina. Following its criteria for SGE
383 exploitations under 30 kW, the BHE should be located at a minimum distance of 3 m
384 from the plot boundaries and separated by at least 6 m.

385 According to this schema, 4 BHEs can be suitable for each plot. These minimum
386 distances are independent of the extracted SGP, so the maximum SGP of 30 kW is
387 assumed to be extracted. This implies that every BHE should extract $30 \text{ (kW)} / 4 = 7.5$
388 kW. For BHEs at 115 m depth, the SGP per unit length would be $7.5 \text{ (kW)} / 115 \text{ (m)} =$
389 65.22 W/m.

390 **Figure 10** shows the thermal plumes produced by these BHEs and the expected
391 thermal interferences. As a consequence of the orientation between the groundwater
392 flow and the cadastral plots, the thermal plumes in plot 15 are aligned; this would
393 reduce BHE efficiency.

394 These thermal plumes represent the thermal contamination with temperature
395 values above 0.5K. By applying the superposition principle, the temperature inside the
396 green areas would be increased by more than 1 K. In cadastral plot 5, the inner thermal
397 influences among BHEs could be neglected. However, the thermal plumes in this plot
398 encroach on the neighboring plots, depleting their energy resource. As a consequence of
399 these thermal interferences, the expected SGE potential of 7.5 kW could not be
400 efficiently extracted from any of these cadastral plots.

401 **4 CONCLUSIONS**

402 The T-I-G^{ER} methodology allows installers to allocate SGE resources in a fair
403 and sustainable manner by taking into account the thermal impacts produced in the
404 subsurface, specifically in groundwater. It integrates the participation of public
405 administration in charge of the SGE management and private installers of SGE
406 exploitations. The steps can be performed with accessible tools: some steps use standard
407 hydrogeological studies and those steps specifically related to SGE use the tools that are
408 provided in this work.

409 As the application in Azul city has shown, the shape and orientation of the
410 cadastral plot is highly relevant when sizing SGE exploitations, especially when
411 groundwater flow exists. If these inputs are not considered, the thermal impacts could
412 affect neighboring BHEs, exceed the plot boundaries and reduce the SGE potential of
413 adjacent plots depleting the energy resource.

414 Ideally, access to required data (groundwater net flow, cadastral data, thermal
415 characteristic curves and thermal plume graphs) should be available through a web map
416 application. The installer would not need advanced knowledge on specific techniques,
417 such as numerical modeling, to ensure the sustainability of SGE resources.

418 **Acknowledgements**

419 This research was supported by the “Dr. Eduardo J. Usunoff” Large Plain
420 Hydrology Institute (IHLLA, Argentina) and the Institute of Environmental Assessment
421 and Water Research (IDÆA-CSIC, Spain). The first autor was funded by the Consejo
422 Nacional de Investigaciones Científicas y Técnicas (CONICET-Argentina).
423 Furthermore, the authors also would like to acknowledge the valuable comments of the
424 two anonymous reviewers for their fruitful suggestions.

425 **5 REFERENCES**

- 426 [1] Z. Abdmouleh, R. A. M. Alammari, and A. Gastli, “Review of policies
427 encouraging renewable energy integration & best practices,” *Renew. Sustain.*
428 *Energy Rev.*, vol. 45, pp. 249–262, 2015.
- 429 [2] A. Zamfir, S. E. Colesca, and R. A. Corbos, “Public policies to support the
430 development of renewable energy in Romania: A review,” *Renew. Sustain.*
431 *Energy Rev.*, vol. 58, pp. 87–106, 2016.
- 432 [3] S. K. Soni, M. Pandey, and V. N. Bartaria, “Ground coupled heat exchangers: A
433 review and applications,” *Renew. Sustain. Energy Rev.*, vol. 47, pp. 83–92, 2015.

- 434 [4] J. W. Lund and T. L. Boyd, "Direct Utilization of Geothermal Energy 2015
435 Worldwide Review," in *Proceedings World Geothermal Congress 2015*, 2015.
- 436 [5] A. Bleicher and M. Gross, "User motivation, energy prosumers, and regional
437 diversity: sociological notes on using shallow geothermal energy," *Geotherm.
438 Energy*, vol. 3, no. 1, p. 12, 2015.
- 439 [6] S. J. Self, B. V. Reddy, and M. a. Rosen, "Geothermal heat pump systems: Status
440 review and comparison with other heating options," *Appl. Energy*, vol. 101, pp.
441 341–348, Jan. 2013.
- 442 [7] P. Hein, O. Kolditz, U. J. Görke, A. Bucher, and H. Shao, "A numerical study on
443 the sustainability and efficiency of borehole heat exchanger coupled ground
444 source heat pump systems," *Appl. Therm. Eng.*, vol. 100, pp. 421–433, 2016.
- 445 [8] T. Vienken, S. Schelenz, K. Rink, and P. Dietrich, "Sustainable intensive thermal
446 use of the shallow subsurface—a critical view on the status Quo," *Groundwater*,
447 vol. 53, no. 3, pp. 356–361, 2015.
- 448 [9] C. Han and X. B. Yu, "Performance of a residential ground source heat pump
449 system in sedimentary rock formation," *Appl. Energy*, vol. 164, pp. 89–98, 2016.
- 450 [10] S. Koochi-Fayegh and M. a. Rosen, "Examination of thermal interaction of
451 multiple vertical ground heat exchangers," *Appl. Energy*, vol. 97, pp. 962–969,
452 2012.
- 453 [11] H. Li, X. Li, and C. K. Soh, "An integrated strategy for sustainable development
454 of the urban underground: From strategic, economic and societal aspects," *Tunn.
455 Undergr. Sp. Technol.*, vol. 55, pp. 67–82, 2016.
- 456 [12] J. van der Gun, A. Aureli, and A. Merla, "Enhancing Groundwater Governance
457 by Making the Linkage with Multiple Uses of the Subsurface Space and Other
458 Subsurface Resources," *Water*, vol. 8, no. 6, p. 222, 2016.
- 459 [13] F. Quattrocchi, E. Boschi, A. Spina, M. Buttinelli, B. Cantucci, and M. Procesi,
460 "Synergic and conflicting issues in planning underground use to produce energy
461 in densely populated countries, as Italy. Geological storage of CO₂, natural gas,
462 geothermics and nuclear waste disposal.," *Appl. Energy*, vol. 101, pp. 393–412,
463 2013.
- 464 [14] A. García-Gil, E. Vázquez-Suñe, E. G. Schneider, J. Á. Sánchez-Navarro, and J.
465 Mateo-Lázaro, "Relaxation factor for geothermal use development – Criteria for
466 a more fair and sustainable geothermal use of shallow energy resources,"
467 *Geothermics*, vol. 56, pp. 128–137, 2015.
- 468 [15] V. Somogyi, V. Sebestyén, and G. Nagy, "Scientific achievements and regulation
469 of shallow geothermal systems in six European countries – A review," *Renew.
470 Sustain. Energy Rev.*, pp. 1–19, 2016.
- 471 [16] AENOR, "UNE 100714-1:2014. Diseño, ejecución y seguimiento de una
472 instalación geotérmica somera [Design, implementation and monitoring of a
473 shallow geothermal installation]." 2014.
- 474 [17] A. García-Gil, E. Vázquez-Suñe, J. Á. Sánchez-Navarro, and J. Mateo Lázaro,
475 "Recovery of energetically overexploited urban aquifers using surface water," *J.
476 Hydrol.*, vol. 531, pp. 602–611, 2015.
- 477 [18] J. Epting, F. Händel, and P. Huggenberger, "Thermal management of an

- 478 unconsolidated shallow urban groundwater body,” *Hydrol. Earth Syst. Sci.*, vol.
479 17, no. 5, pp. 1851–1869, May 2013.
- 480 [19] V. L. Freedman, S. R. Waichler, R. D. Mackley, and J. a. Horner, “Assessing the
481 thermal environmental impacts of an groundwater heat pump in southeastern
482 Washington State,” *Geothermics*, vol. 42, pp. 65–77, 2012.
- 483 [20] A. García-Gil, E. Vázquez-Suñe, E. G. Schneider, J. Á. Sánchez-Navarro, and J.
484 Mateo-Lázaro, “The thermal consequences of river-level variations in an urban
485 groundwater body highly affected by groundwater heat pumps.,” *Sci. Total
486 Environ.*, vol. 485–486, pp. 575–87, Jul. 2014.
- 487 [21] T. Arola, L. Eskola, J. Hellen, and K. Korkka-Niemi, “Mapping the low enthalpy
488 geothermal potential of shallow Quaternary aquifers in Finland,” *Geotherm.
489 Energy*, vol. 2, no. 1, p. 9, 2014.
- 490 [22] A. García-Gil, E. Vázquez-Suñe, M. M. Alcaraz, A. S. Juan, J. Á. Sánchez-
491 Navarro, M. Montlleó, G. Rodríguez, and J. Lao, “GIS-supported mapping of
492 low-temperature geothermal potential taking groundwater flow into account,”
493 *Renew. Energy*, vol. 77, pp. 268–278, May 2015.
- 494 [23] A. Galgaro, E. Di Sipio, G. Teza, E. Destro, M. De Carli, S. Chiesa, A. Zarrella,
495 G. Emmi, and A. Manzella, “Empirical modeling of maps of geo-exchange
496 potential for shallow geothermal energy at regional scale,” *Geothermics*, vol. 57,
497 pp. 173–184, 2015.
- 498 [24] A. Santilano, A. Donato, A. Galgaro, D. Montanari, A. Menghini, A. Viezzoli, E.
499 Di Sipio, E. Destro, and A. Manzella, “An integrated 3D approach to assess the
500 geothermal heat-exchange potential: The case study of western Sicily (southern
501 Italy),” *Renew. Energy*, vol. 97, pp. 611–624, 2016.
- 502 [25] A. Casasso and R. Sethi, “Assessment and mapping of the shallow geothermal
503 potential in the province of Cuneo (Piedmont, NW Italy),” *Renew. Energy*, vol.
504 102, pp. 306–315, 2017.
- 505 [26] M. Alcaraz, A. García-Gil, E. Vázquez-Suñe, and V. Velasco, “Advection and
506 dispersion heat transport mechanisms in the quantification of shallow geothermal
507 resources and associated environmental impacts,” *Sci. Total Environ.*, vol. 543,
508 pp. 536–546, 2016.
- 509 [27] K. Schiel, O. Baume, G. Caruso, and U. Leopold, “GIS-based modelling of
510 shallow geothermal energy potential for CO₂ emission mitigation in urban
511 areas,” *Renew. Energy*, vol. 86, pp. 1023–1036, 2016.
- 512 [28] M. Alcaraz, A. García-Gil, E. Vázquez-Suñe, and V. Velasco, “Use rights
513 markets for shallow geothermal energy management,” *Appl. Energy*, vol. 172,
514 pp. 34–46, 2016.
- 515 [29] C. S. Blázquez, A. F. Martín, P. C. García, L. S. Sánchez Pérez, and S. J. del
516 Caso, “Analysis of the process of design of a geothermal installation,” *Renew.
517 Energy*, vol. 89, pp. 188–199, 2016.
- 518 [30] A. Casasso and R. Sethi, “G.POT: A quantitative method for the assessment and
519 mapping of the shallow geothermal potential,” *Energy*, vol. 106, pp. 765–773,
520 2016.
- 521 [31] G. de. Marsily, *Quantitative hydrogeology: groundwater hydrology for
522 engineers*. Academic Press, 1986.

- 523 [32] M. Li and A. C. K. Lai, "Review of analytical models for heat transfer by vertical
524 ground heat exchangers (GHEs): A perspective of time and space scales," *Appl.*
525 *Energy*, vol. 151, pp. 178–191, 2015.
- 526 [33] T. Metzger, S. Didierjean, and D. Maillet, "Optimal experimental estimation of
527 thermal dispersion coefficients in porous media," *Int. J. Heat Mass Transf.*, vol.
528 47, pp. 3341–3353, 2004.
- 529 [34] N. Molina-Giraldo, P. Bayer, and P. Blum, "Evaluating the influence of thermal
530 dispersion on temperature plumes from geothermal systems using analytical
531 solutions," *Int. J. Therm. Sci.*, vol. 50, no. 7, pp. 1223–1231, Jul. 2011.
- 532 [35] A. Capozza, M. De Carli, and A. Zarrella, "Investigations on the influence of
533 aquifers on the ground temperature in ground-source heat pump operation," *Appl.*
534 *Energy*, vol. 107, pp. 350–363, 2013.
- 535 [36] M. Verdoya and P. Chiozzi, "Influence of groundwater flow on the estimation of
536 subsurface thermal parameters," *Int. J. Earth Sci.*, pp. 1–8, 2016.
- 537 [37] M. Bonte, W. F. M. Röling, E. Zaura, P. W. J. J. Van Der Wielen, P. J.
538 Stuyfzand, and B. M. Van Breukelen, "Impacts of shallow geothermal energy
539 production on redox processes and microbial communities," *Environ. Sci.*
540 *Technol.*, vol. 47, no. 24, pp. 14476–14484, 2013.
- 541 [38] A. García-Gil, J. Epting, C. Ayora, E. Garrido, E. Vázquez-Suñé, P.
542 Huggenberger, and A. C. Gimenez, "A reactive transport model for the
543 quantification of risks induced by groundwater heat pump systems in urban
544 aquifers," *J. Hydrol.*, vol. 542, pp. 719–730, 2016.
- 545 [39] J. C. Choi, J. Park, and S. R. Lee, "Numerical evaluation of the effects of
546 groundwater flow on borehole heat exchanger arrays," *Renew. Energy*, vol. 52,
547 pp. 230–240, Apr. 2013.
- 548 [40] J. Schön, *Physical Properties of Rocks: A Workbook*. Amsterdam: Elsevier B.V.,
549 2011.
- 550 [41] M. E. Zabala, M. Manzano, and L. Vives, "The origin of groundwater
551 composition in the Pampeano Aquifer underlying the Del Azul Creek basin,
552 Argentina," *Sci. Total Environ.*, vol. 518–519, pp. 168–188, 2015.
- 553 [42] G. Cazenave, F. Peluso, L. Vives, and E. Usunoff, "Aplicación de modelos de
554 transporte de solutos para el análisis del riesgo sanitario en aguas subterráneas.
555 Caso de Azul, Argentina [Application of solute transport models for health risk
556 analysis in groundwater. Case study of Azul, Argentine]," in *XX Congreso*
557 *Nacional del Agua*, 2005.
- 558 [43] G. Cazenave and L. S. Vives, "Modelo de transporte de solutos en aguas
559 subterráneas de la ciudad de Azul, Provincia de Buenos Aires, Argentina
560 [Groundwater solute transport model of Azul city, Buenos Aires Province,
561 Argentine]," *Cuad. del CURIHAM*, vol. 10, pp. 33–43, 2004.
- 562 [44] M. E. Zabala, M. Manzano, and L. Vives, "Assessment of processes controlling
563 the regional distribution of fluoride and arsenic in groundwater of the Pampeano
564 Aquifer in the Del Azul Creek basin (Argentina)," *J. Hydrol.*, 2016.
- 565 [45] L. Romero, H. Alonso, P. Campano, L. Fanfani, R. Cidu, C. Dadea, T. Keegan, I.
566 Thornton, and M. Farago, "Arsenic enrichment in waters and sediments of the
567 Rio Loa (Second Region, Chile)," *Appl. Geochemistry*, vol. 18, no. 9, pp. 1399–

- 568 1416, Sep. 2003.
- 569 [46] M. Bonte, B. M. van Breukelen, and P. J. Stuyfzand, “Temperature-induced
570 impacts on groundwater quality and arsenic mobility in anoxic aquifer sediments
571 used for both drinking water and shallow geothermal energy production,” *Water*
572 *Res.*, vol. 47, no. 14, pp. 5088–5100, 2013.
- 573 [47] “Cadastral plots distribution. Government of Argentine Republic.” [Online].
574 Available: <https://www.carto.arba.gov.ar/>. [Accessed: 08-Jul-2016].
- 575
- 576

577 **Figure 1.** Sketch of synthetic Thermal Characteristic Curve (TCC). The TCC represents the
578 relation between the SGP and the length of its thermal impacts in the subsurface.

579 **Figure 2.** Sketch of the synthetic thermal plume graph (TPG). The TPG represents the size and
580 dimensions of the thermal impacts for a particular BHE in a plot.

581 **Figure 3.** Length (L) and width (W) dimensions of cadastral plots with respect to groundwater
582 flow.

583 **Figure 4.** Location map of Azul city in Pampean plains.

584 **Figure 5.** Regional piezometry, groundwater flow net and Darcy velocity in Azul city.

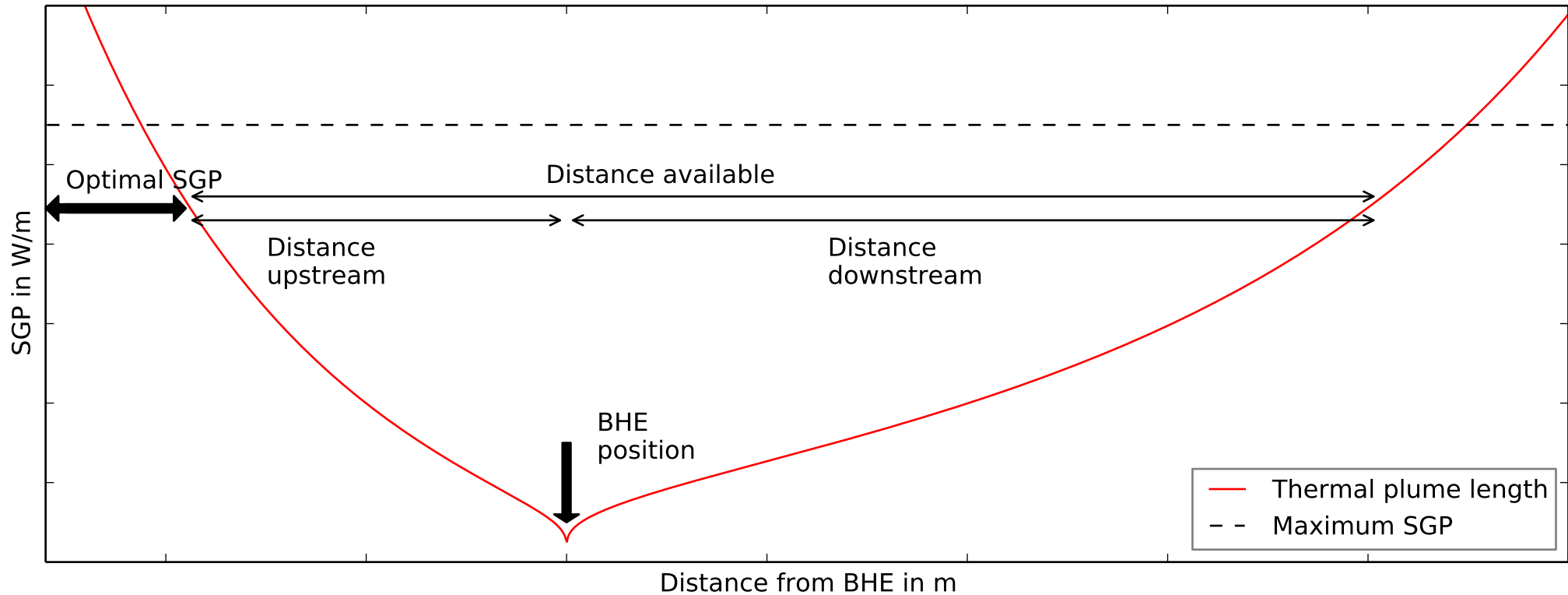
585 **Figure 6.** Location of the block and the cadastral plots under study. The dimensions W and L that
586 are required to size SGE exploitation are remarked for cadastral plots 5 and 15. These dimensions are
587 defined according to the groundwater flow direction.

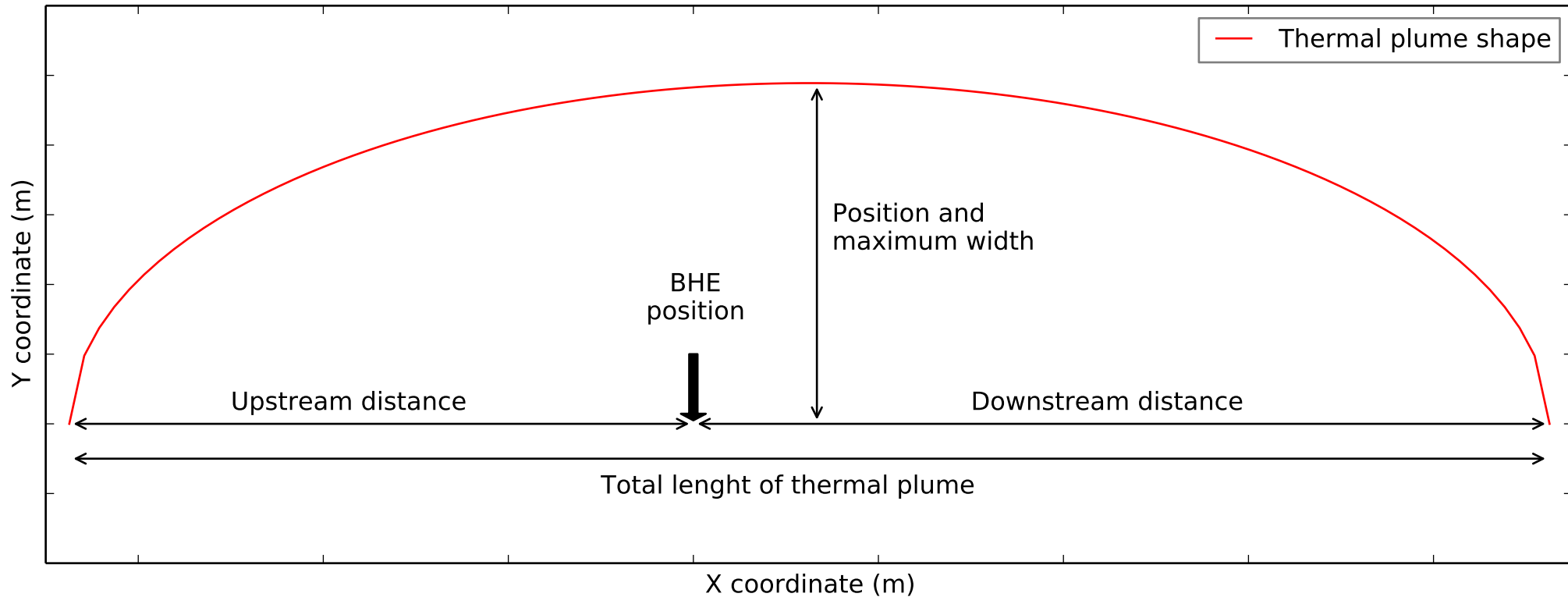
588 **Figure 7.** Thermal characteristic curve for cadastral plots 15 and 5. The limiting dimensions for
589 each plot are represented along with the corresponding SGP.

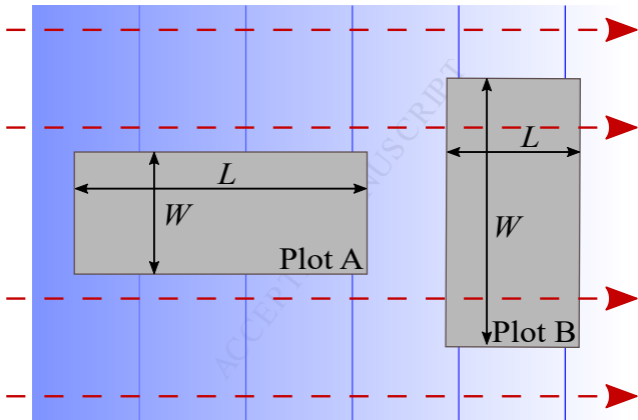
590 **Figure 8.** Thermal plume graphs for the SGE exploitations in cadastral plots 15 and 5. This
591 graph complements the TCC when drawing the thermal plume.

592 **Figure 9.** Configuration of the BHE exploitations in cadastral plots 15 and 5. To extract a similar
593 SGP from these different plots, the less favourable plot (cadastral plot 5) requires more BHEs.

594 **Figure 10.** Thermal affections that would be produced following the existing regulations in the
595 reference scenario. These thermal plumes can deplete SGE of the plot with inner thermal influences and
596 the neighbouring plots with outer thermal influences.

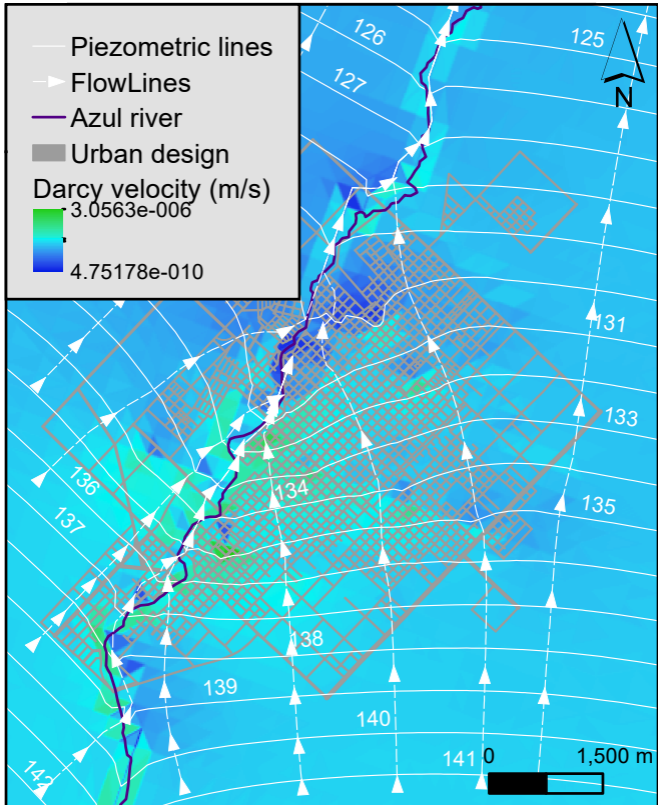




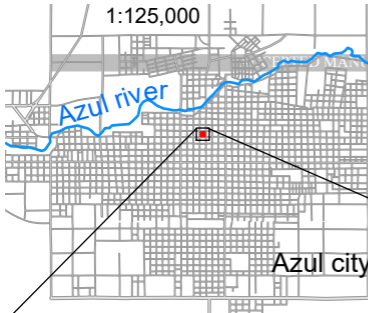


-- -- ➤ *Groundwater stream flow*





1:125,000



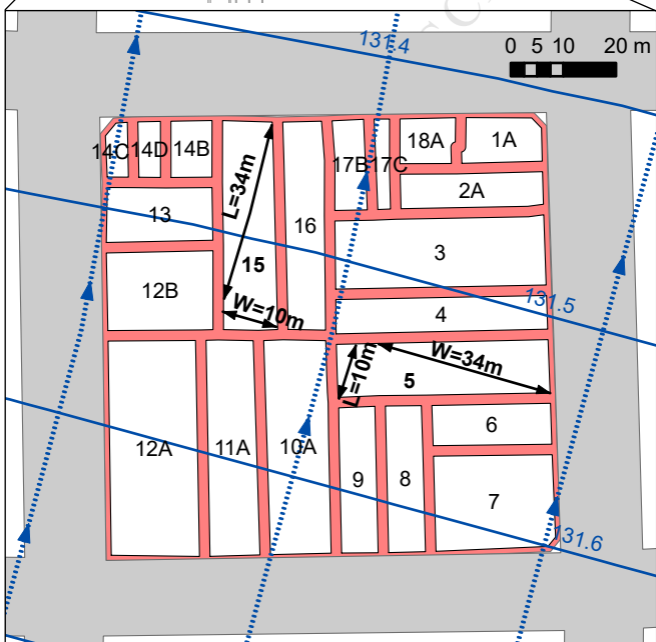
Urban design

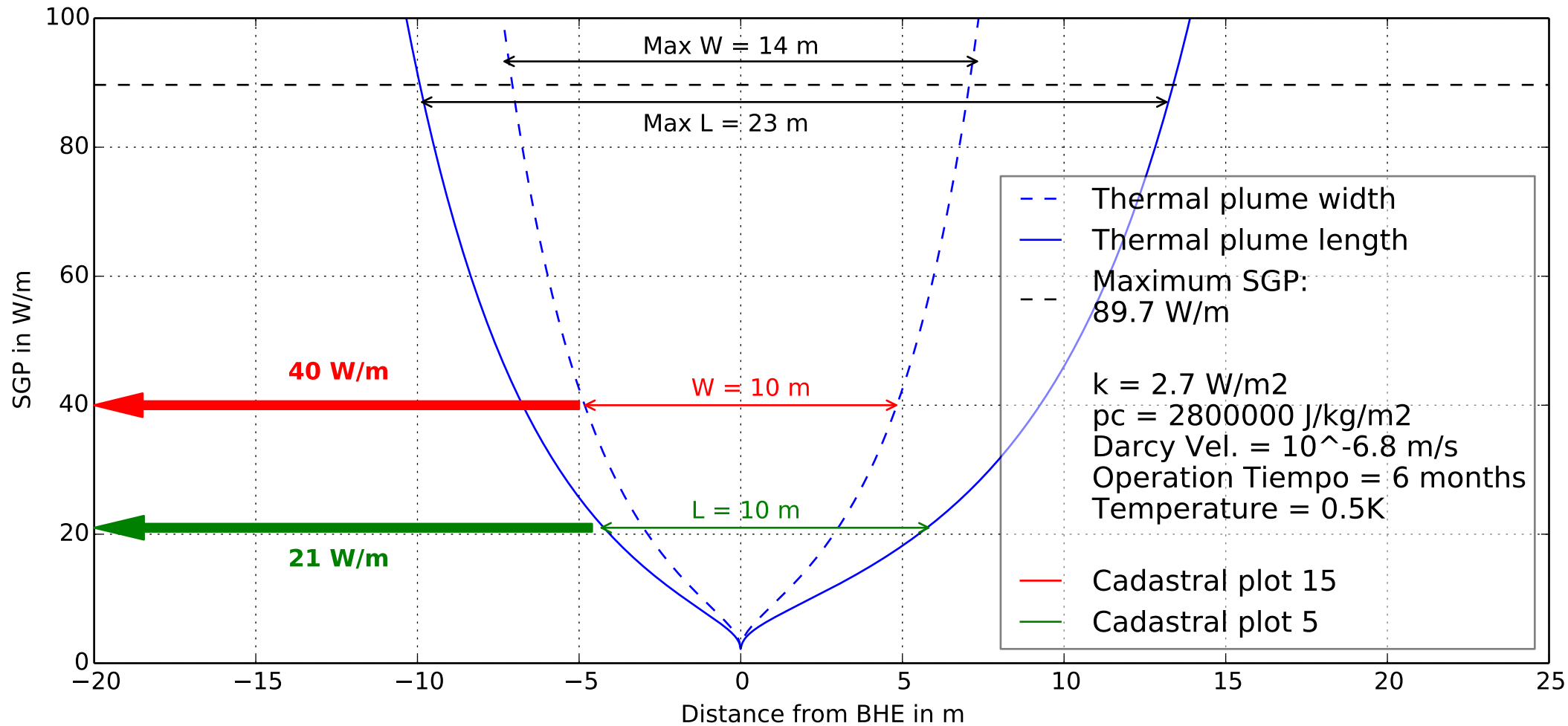
Block 186

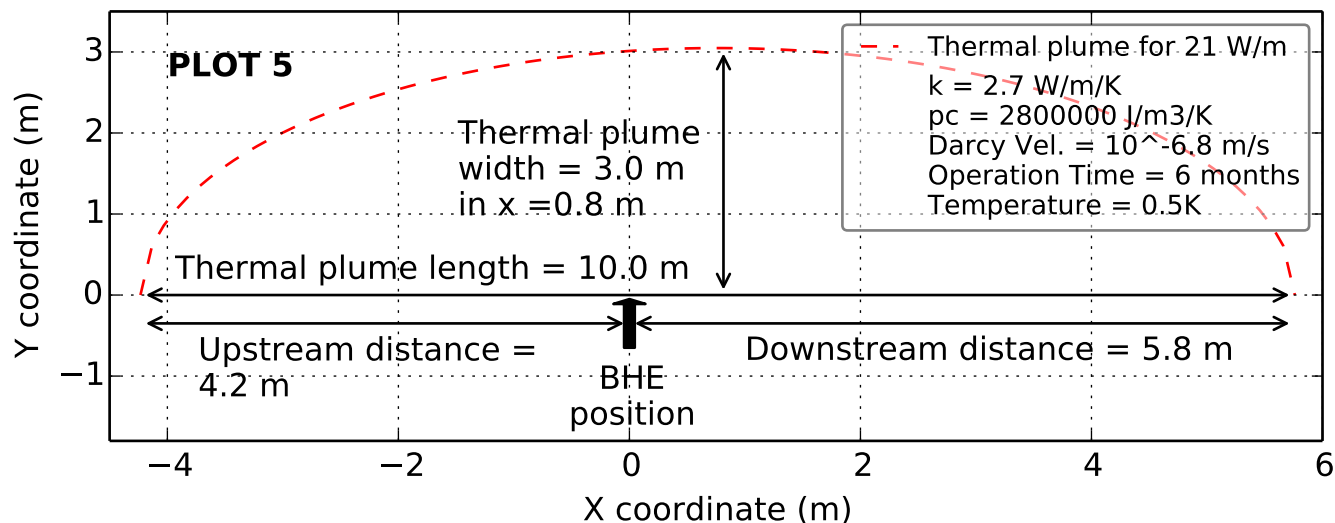
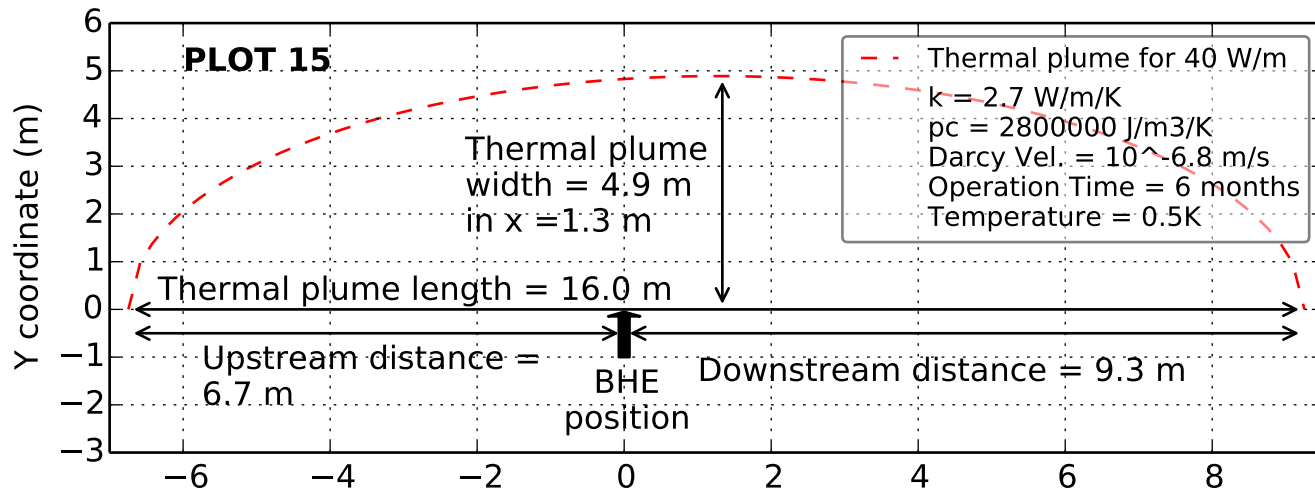
Cadastral plots

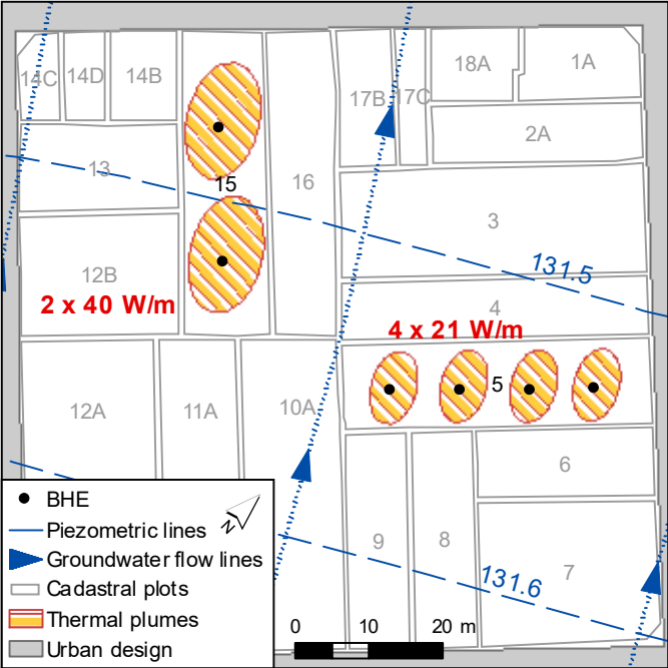
Piezometric lines

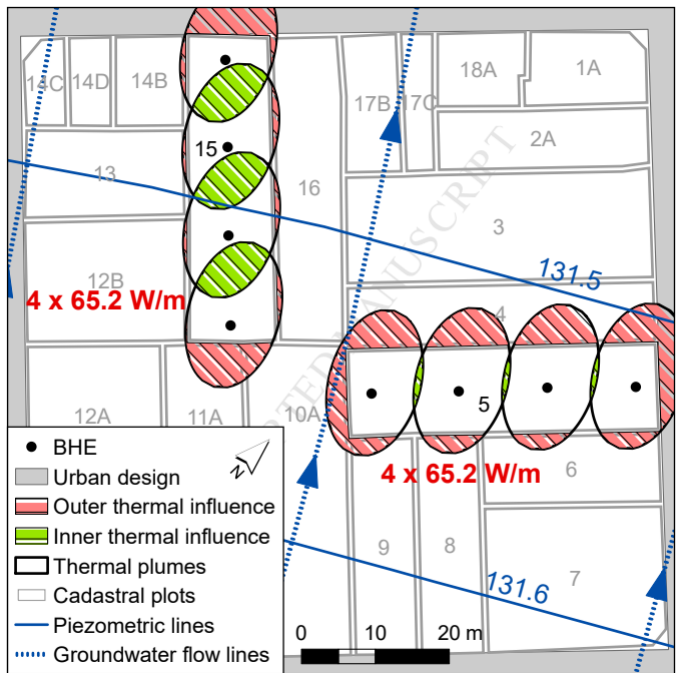
Groundwater flow lines











Highlights:

- A simple method is proposed to sustainably size shallow geothermal exploitations
- A graph relates the maximum shallow geothermal potential and its thermal impacts
- It is based on local thermal and groundwater properties and on the plot orientation

c	Specific heat capacity (J/kg/K)
i	hydraulic gradient (m/m)
K	Hydraulic conductivity (m/s)
L	Maximum length available inside the cadastral plot (m)
q	Groundwater velocity or Darcy velocity (m/s)
q_L	Heat flow rate per unit length of the borehole (W/m)
S	Heat source/sink term (W/m ³)
t	Elapsed time (s)
ΔT	Temperature change produced in the ground (K)
T	Average temperature of the porous medium (K)
W	Maximum width inside the cadastral plot (m)
x/y	Cartesian coordinates (m)

Greek symbols

ϕ	Integration variable
ρc	volumetric heat capacity of the subsurface (J/m ³ /K)
$\rho_w c_w$	volumetric heat capacity of water (J/m ³ /K)
$\lambda_{x/y}$	Effective thermal conductivity (W/m/K)